Supplementary Information

Spinach RNA aptamer detects lead (II) with high selectivity

Saurja DasGupta[1], Sandip A. Shelke[2], Nan-sheng Li[2], Joseph A. Piccirilli*[1,2]

[1]Department of Chemistry, The University of Chicago, Chicago, IL, 60637, USA.
[2]Department of Biochemistry and Molecular Biology, The University of Chicago, Chicago, IL, 60637, USA.

Experimental Methods

Construct preparation, RNA synthesis and purification, and other chemicals. The sequence of the Spinach sensor RNA is: 5'-GGGGAGAAGGACGGGUCCAGUGCGAAACACGCA CUGUUGAGUAGAGUGUGAGCUCCC-3'. DNA cloning, synthesis (by *in-vitro* transcription) and purification of RNA by FPLC was performed following the procedure outlined in ref. 9a (Huang *et al.*). DFHBI was synthesized by following a previously reported scheme in ref. 9a (Huang *et al.*). Metal salts like $Pb(CH_3COO)_2.3H_2O$ (used as a source of Pb^{2+} for all experiments) were purchased from Sigma-Aldrich (ACS grade).

Stability Assays. Stability of the spinach sensor was assayed at different conditions relevant to possible real life contexts. For tap water assays, the sensor was incubated with 10 μM Pb^{2+} at 25 ^oC in tap water for 15, 90, 180 minutes and 7 days and at 37 ^oC overnight (~16 h). For pH assays, the sensor was incubated with 10 μM Pb^{2+} at 25 ^oC for 60 minutes in buffers with pH from 3 to 11. Aliquots were mixed with standard loading dye and loaded on an analytical dPAGE. Gel was stained with ethidium bromide for visualization under UV.

Fluorescence Assays. Purified RNA was ethanol precipitated twice and refolded in the presence of a folding buffer containing 10 mM Tris (pH 7.5) and 5 mM Mg^{2+} (heating at 90 ^oC for two minutes in water followed incubation on ice for 5 minutes; then heating at 50 ^oC for 30 minutes in presence of 5 mM Mg^{2+} followed incubation on ice for 5 minutes). All experiments were performed in the same buffer conditions. For metal binding assays, fluorophore DFHBI was added to the RNA and incubated at 37 ^oC for 10 minutes.

Concentrations of RNA and DFHBI used for sensitivity and selectivity assays were 5 µM and 20 µM, respectively, unless otherwise mentioned. Different concentrations of Pb^{2+} (for sensitivity and selectivity assays) or other metal ions (for selectivity assays) were added and incubated at 37 °C for 15 minutes. For DFHBI binding assays, RNA was taken in 30 nM concentration. For tap water experiments, 100 nM RNA and 1 µM DFHBI was used. Fluorescence emission was measured using a Fluorolog-3 spectrofluorometer equipped with a thermo-controller (Horiba Inc.) at an excitation wavelength of 468 nm (Fig. S14a) and emission range of 490-520 nm (Figs S6b, S14b) with a slit width of 5 nm; results were the average of three consecutive independent measurements and each measurement was performed in triplicate (the data points represent the average of these triplicate measurements). All measurements were done at 25 °C. Data were normalized and plotted in Microsoft Excel and Origin.

RNA-metal ion and RNA-fluorophore affinity measurements. Binding affinities of Pb^{2+} and Ca^{2+} to Spinach RNA were determined by measuring the increase in fluorescence as a function of concentration of these cations in the presence of 100 nM RNA and 1 µM DFHBI and 5 µM RNA and 20 µM DFHBI, respectively. Determination of binding affinity of the fluorophore to metal bound RNA was performed in presence of 10 µM Pb^{2+} or 50 mM Ca^{2+} and 30 nM RNA. For each concentration of fluorophore, a background signal for the fluorophore without RNA in the buffer was also measured and subtracted from the signal observed for the fluorophore with RNA. Curves were fitted to the Hill equation: $y= (C_0 + Cmax*x^{n)}/(K_D^n + x^n)$. All measurements were done at 25 °C. Data were normalized and plotted in Origin.

Circular Dichroism (CD) Measurements. Measurements were performed using a JASCO-1500 CD Spectrometer. Samples were prepared same way as in the case of fluorescence experiments. Concentrations of RNA and DFHBI were 5 µM and 20 µM, respectively. Three scans from 180 to 320 nm at 1 nm intervals were accumulated with a scan rate of 100 nm min^{-1} and averaged (Path length=1 mm). All measurements were done at 25 °C. Data were plotted in Microsoft Excel.

Mutational studies on the G-quadruplex region. The following mutants were used:

ΔQ1: 5'-GGGGAGAAGCACGUGUCCAGUGCGAAACACGCACUGUUGACUAGAU
UGUGAGCUCCC-3'

ΔQ2: 5'-GGGGAGAACGACUGGUCCAGUGCGAAACACGCACUGUUGAGUACAG

UUUGAGCUCCC-3'

The wild-type sequence (the sequence of the Spinach sensor) used as a positive control was:

WT: 5'-GGGGAGAAGGACGGGUCCAGUGCGAAACACGCACUGUUGAGUAGAGU GUGAGCUCCC-3'

The G-quadruplex guanines are highlighted in blue and the G mutations are highlighted in red. Fluorescence experiments were performed as indicated above. Concentrations of RNA and DFHBI were 5 μM and 20 μM, respectively. For each construct (wild-type and two mutants), the background signal without Pb^{2+} was subtracted from the signal observed with Pb^{2+}. Data were plotted in Microsoft Excel.

ICP-MS Analysis of tap water. Data were collected using an Agilent 7700x inductively coupled plasma mass spectrometer (ICP-MS) using ICP-MS MassHunter version B01.03. Samples were diluted in a 2% HNO_3 matrix and analyzed against a 8 point standard curve (for Pb^{2+}) or 5 point standard curve (for Na^+, Ca^{2+}, and K^+) over the range from 0.05 ppb to 25 ppb (for Pb) or 0.1 ppm to 1 ppm (for Na^+, Ca^{2+}, and K^+). For all analyses, the correlation coefficient was > 0.9990 for all analytes of interest. The signal was normalized against a Tb 159 internal standard. Data collection was performed in Spectrum Mode with five replicates per sample and 100 sweeps per replicate. Each sample was analyzed three times for consistency.

Supplementary Table

Table S1. Comparison of Spinach RNA sensor with DNA-based sensors reported in literature. (Increase or decrease in signal is indicated in brackets)

Mechanism of action	Detection method	Sensitivity (Detection Limit)	Selectivity (w.r.t. the most interfering cation)	Incubation time	Linear Range	Reference
Pb^{2+} induced formation of G-quadruplex	Fluorescence *(Increase)*	6 nM	~ 17000 fold	15 min	5-500 nM	This work
	Fluorescence *(Decrease)*	1.0 nM	~ 5 fold	30 min	5 nM-1 µM	(a)
	Fluorescence *(Decrease)*	0.4 nM	~ 15 fold	15 min	0.5 – 500 nM	(b)
	Fluorescence *(Increase)*	5 nM	~ 30 fold	2 hours	20 nM-1 µM	(c)
	Fluorescence *(Decrease)*	~4 nM	~ 3 fold	5 min	0-960 nM	(d)
	Fluorescence *(Anisotropy)*	1.0 nM	~ 50 fold	30 min	10 nM-2 µM	(e)
	Electrochemistry *(Increase)*	0.4 nM	~4 fold	10 min	1 nM-1 µM	(f)
	Electrochemistry *(Decrease)*	0.075 nM	~ 5 fold	30 min	0.1 nM-0.1 µM	(g)
	Electrochemistry *(Increase)*	3.3 pM	-	-	0.01 – 160 nM	(h)
	Surface Plasmon resonance (SPR)	>0.4 nM	-	5-6 hours	-	(i)
Pb^{2+} induced formation of G-quadruplex DNAzyme	Fluorescence *(Increase)*	0.4 nM	~4 fold	2-3 hours	0-1 µM	(j)
	Fluorescence *(Increase)*	0.05 nM	~ 40 fold	2 hours	0-100 nM	(k)
	Colorimetry *(Decrease)*	32 nM	~ 6 fold	1-2 hours	100 nM-10 µM	(l)
	Chemiluminiscence *(Decrease)*	1 nM			10^{-9}-$10^{-6.5}$ M	
	Electrochemistry *(Decrease)*	0.5 nM	-	4 hours	-	(m)
	Surface Plasmon Resonance	~ 0.005 pM	~ 25 fold	-	-	(n)
	Electrochemistry	0.1 nM	~ 6 fold			

	(Decrease)					
Pb^{2+} DNAzyme catalyzed RNA cleavage	Fluorescence *(Increase)*	3.7 nM	~ 6000 fold	6 min	-	(o)
	Fluorescence *(Increase)*	-	~ 40 fold	15 min	10 nM-4 μM	(p)
	Fluorescence *(Increase)*	~ 3 nM	~ 500 fold	30 min	5-100 nM	(q)
	Electrochemistry *(Decrease)*	0.9 pM	~ 2 fold	1 hour	2 pM-1nM	(r)
	Electrochemistry *(Increase)*	0.6 mM	~ 50 fold	1 hour	1 nM-1 μM	(s)

References for Table S1

(a) L. Guo, *et al. Biosens. Bioelectron.*, 2012, **35**, 123-127
(b) W. Wang, Y. Jin, Y. Zhao, X. Yue and C. Zhang, *Biosens. Bioelectron.*, 2013, **41**, 137-142
(c) T. Li, S. Dong and E. Wang, *J. Am. Chem. Soc.* 2010, **132**, 13156-13157
(d) S. Zhan *et al. RSC Adv*. 2013, **3**, 16962-16966.
(e) D. Zhang, L. Yin, Z. Meng, A. Yu, L. Guo and H. Wang, *Anal. Chim, Acta.* 2014, **812**, 161-167
(f) F. Li, Y. Feng, C. Zhao and B. Tang, *Chem. Commun.*, 2011, **47**, 11909-11911
(g) F. Li, L. Yang, M. Chen, P. Li and B. Tang, *Analyst.*, 2013, **138**, 461-466.
(h) M. Liu *et al. Environ. Sci. Technol.* 2010, **44**, 4241-4246
(i) S. Cheng, *et al*. *Biosens. Bioelectron.*, 2014, **53**, 479-485
(j) C-L. Li, K-T. Liu, Y-W. Lin and H-T. Chang, *Anal. Chem.*, 2011, **83**, 225-23
(k) C-L. Li, C-C. Huang, W-H. Chen, C-K. Chiang and H-T. Chang, *Analyst*, 2012, **137**, 5222-5228
(l) T. Li, E. Wang and S. Dong, *Anal. Chem.*, 2010, **82**, 1515-1520
(m) F. Li, L. Yang, M. Chen, Y. Qian and B. Tang, *Biosens. Bioelectron.*, 2013, **41**, 903-906
(n) G. Pelossof, R. Tel-Vered and I. Willner, *Anal. Chem.*, 2012, **84**, 3703-3709
(o) T. Lan, K. Furuya and Y. Lu, *Chem. Commun.*, 2010, **46**, 3896-3898
(p) Y. Lu, J. Liu, J. Li, P. J. Bruesehoff, C. M.-B. Pavot and A. K. Brown, *Biosens. Bioelectron.*, 2003, **41**, 529-540
(q) H. Li, Q. Zhang, Y. Cai, D-M. Kong, H-X. Shen, *Biosens. Bioelectron.*, 2012, **34**, 159-164
(r) A. Gao, C-X. Tang, X-W. He and X-B. Yin, *Analyst*, 2013, **138**, 263-268
(s) H. Zhang, B. Jiang, Y. Xiang, J, Su, Y. Chai and R. Yuan, *Biosens. Bioelectron.*, 2011, **41**, 529-540

Supplementary Figures

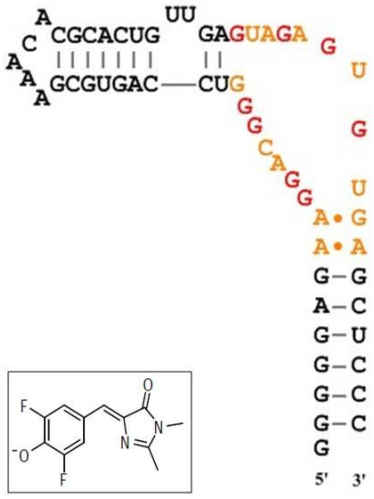

Figure S1. Secondary structure of the Spinach RNA and the fluorophore, DFHBI (boxed) used in the Spinach sensor. Gs involved in the quadruplex are shown in red.

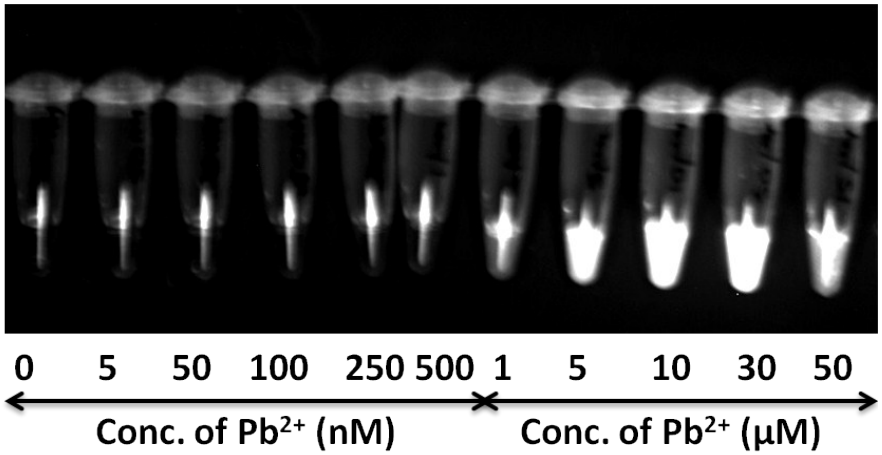

Figure S2. Spinach sensor gives a strong fluorescence signal at Pb^{2+} concentrations ≥ 1 µM as observed under UV light. RNA and DFHBI concentrations were 5 µM and 20 µM respectively.

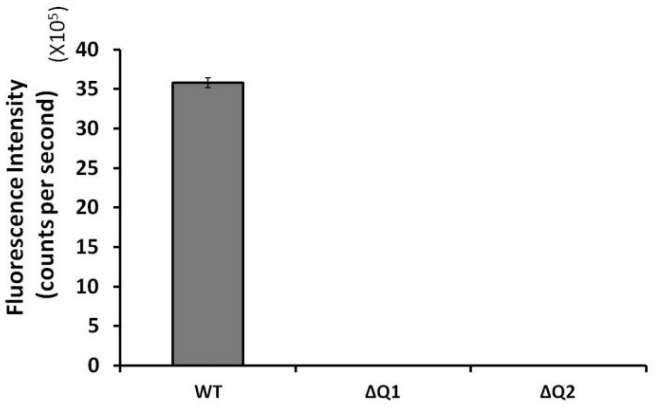

Figure S3. Mutations of G-quadruplex nucleotides abolish Pb^{2+}- induced Spinach fluorescence. WT Spinach sensor shows strong fluorescence signal in presence of 10 μM Pb^{2+}, but quadruplex mutants of the sensor, ΔQ1 and ΔQ2 do not show fluorescence over background. RNA and DFHBI concentrations were 5 μM and 20 μM respectively.

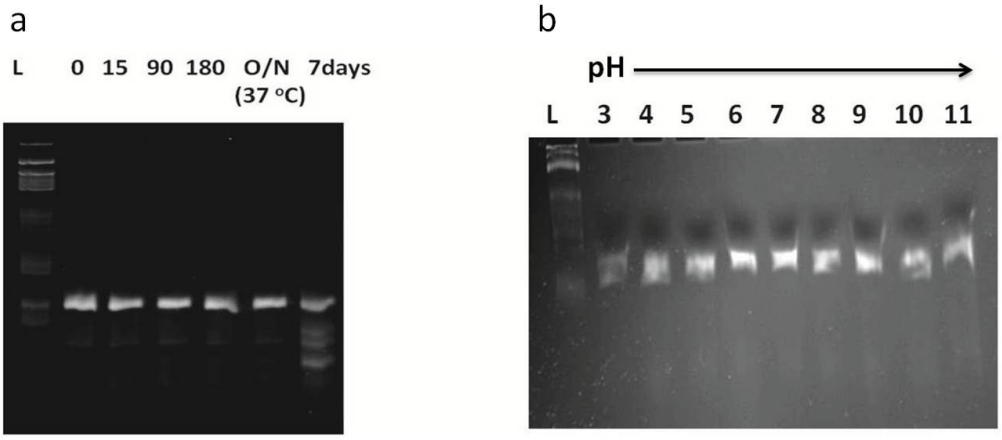

Figure S4. Stability of sensor in real life contexts. (a) Denaturing polyacrylamide gel electrophoresis (dPAGE) showing the stability of Spinach sensor in tap water in the presence of 10 μM Pb^{2+} incubated at 25 °C unless otherwise mentioned. Tested time points are 15, 90, 180 minutes, overnight (O/N) and 7 days. The RNA aptamer shows minimal cleavage in the presence of 10 μM Pb^{2+} in tap water after incubation at 37 °C overnight. (b) dPAGE showing the stability of Spinach sensor in different pH (3-11) incubated with 10 μM Pb^{2+} at 25 °C for 60 minutes . L denotes low-range ssRNA ladder.

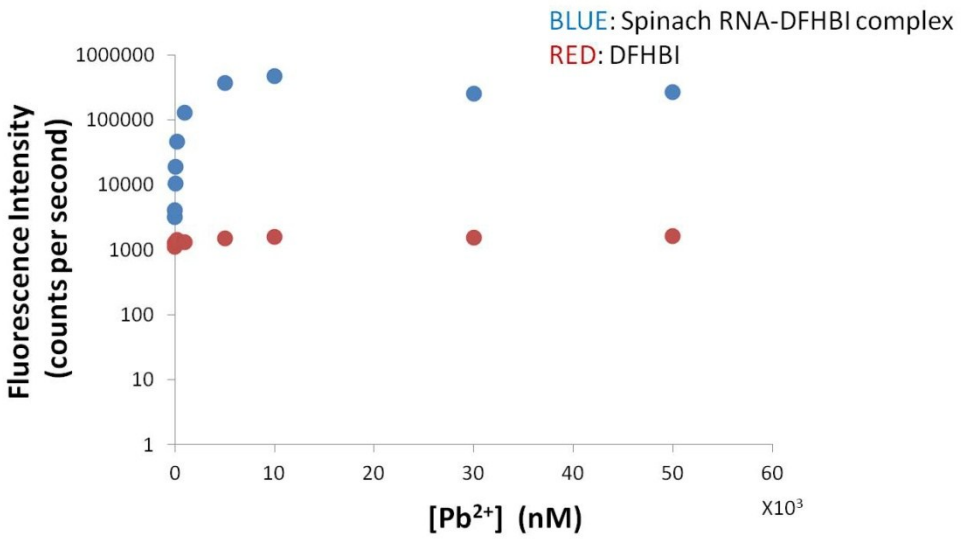

Figure S5. Fluorescence signal of DFHBI with different concentrations of Pb^{2+} (5 nM-50 µM) in presence (blue) or absence (red) of spinach RNAFluorescence signal remains constant over the wide concentration range of Pb^{2+} in the absence of RNA, but shows a sharp rise in its presence. . RNA and DFHBI concentrations were 5 µM and 20 µM, respectively.

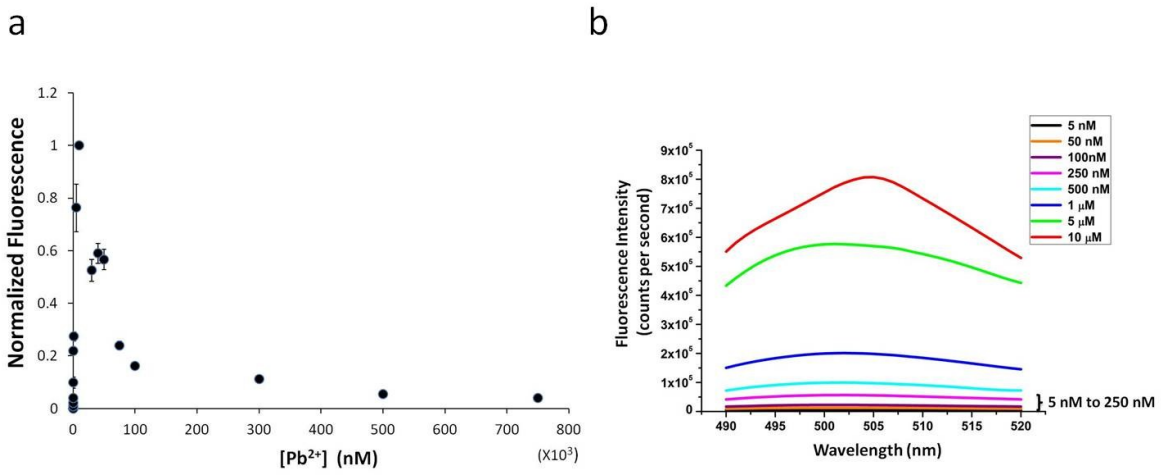

Figure S6. Fluorescence response of the Spinach sensor to different concentrations of Pb^{2+}. (a) Complete plot for Fig. 3 showing response of Spinach sensor to increasing concentrations of Pb^{2+} (5 nM-750 µM). Fluorescence decreases after 10 µM. (b) Fluorescence spectra in the region 490 nm–520 nm (excitation wavelength 468 nm). The color code indicates concentrations of Pb^{2+}. RNA and DFHBI concentrations were 5 µM and 20 µM, respectively.

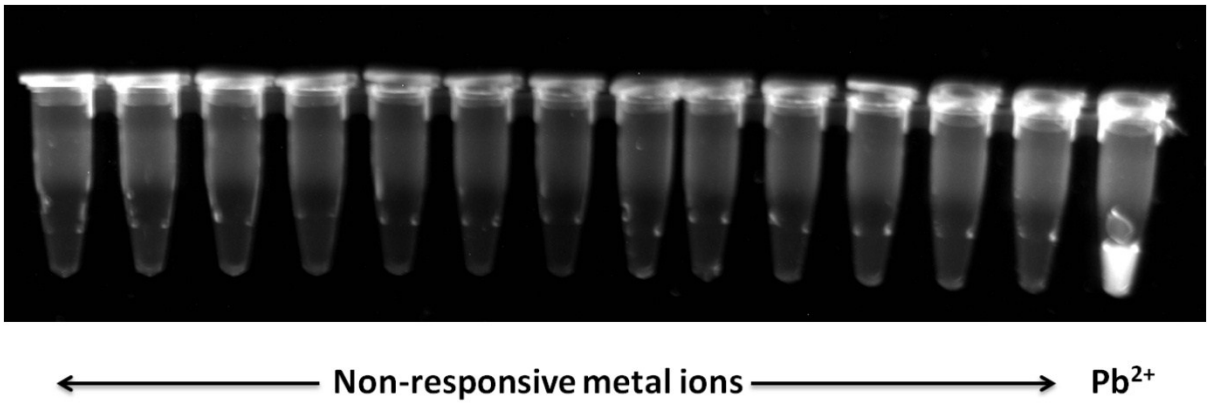

Figure S7. Pb^{2+} (10 μM) activates DFHBI fluorescence in the presence of Spinach RNA. Other metals (Ag^{+}, Co^{2+}, Cr^{3+}, Cd^{2+}, Na^{+}, Cu^{2+}, Hg^{2+}, Fe^{2+}, Mn^{2+}, Ni^{2+}, Zn^{2+} at 300 μM and K^{+}, Ca^{2+} at 30 μM) show no fluorescence activation. RNA and DFHBI concentrations were 5 μM and 20 μM respectively.

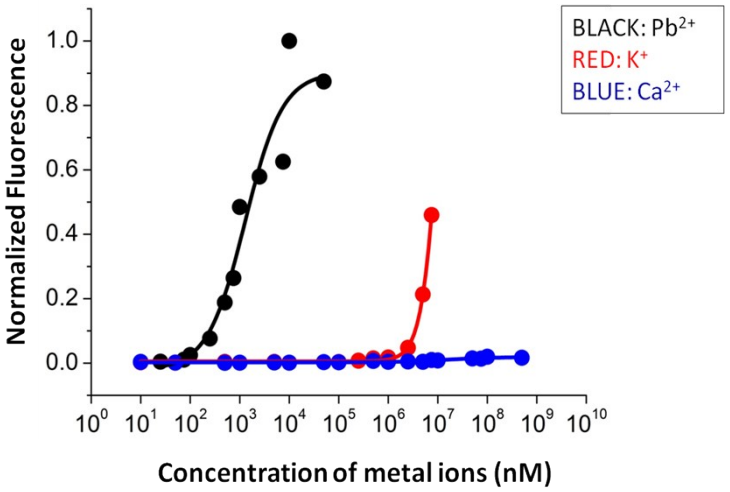

Figure S8. Concentration dependence of Spinach fluorescence activation by Pb^{2+}, K^{+}, Ca^{2+} at low RNA/DFHBI concentrations. RNA and DFHBI concentrations were 100 nM and 1 μM, respectively.

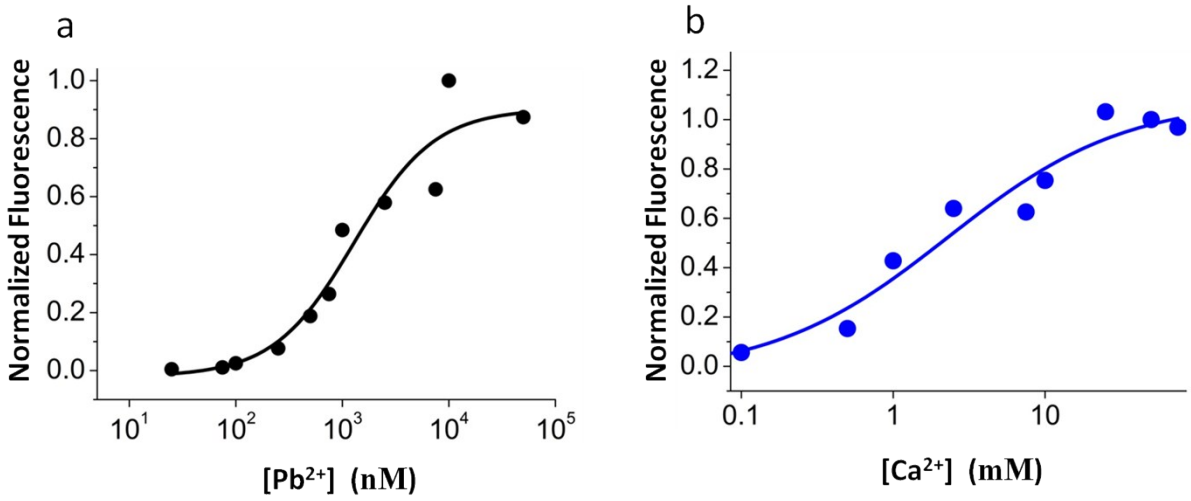

Figure S9. Concentration dependence of Spinach fluorescence activation by Pb^{2+} and Ca^{2+}. Pb^{2+} shows a strong affinity towards Spinach RNA with an apparent K_D of 1.29 ± 0.45 µM (n=1.5±0.4) (a), whereas Ca^{2+} shows a weaker binding affinity with an apparent K_D of 2.29 ± 1.12 mM (n=0.7±0.3). (b) Concentrations of RNA and DFHBI were 100 nM and 1 µM, respectively, for the Pb^{2+} assays and 5 µM and 20 µM, respectively, for Ca^{2+} assays.

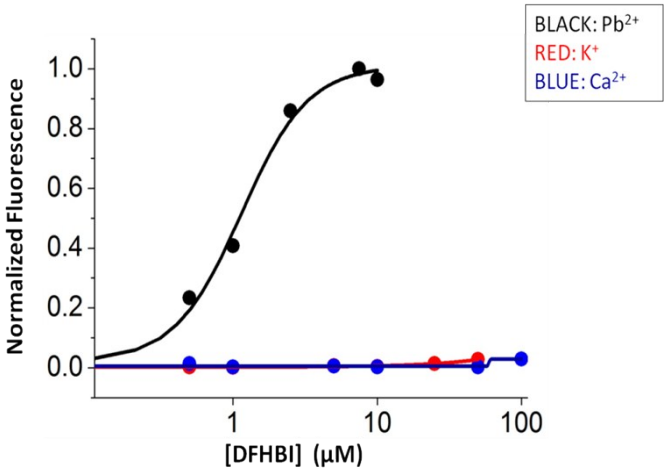

Figure S10. DFHBI dependence of fluorescence activation by Spinach at low concentrations of cations. At 10 µM concentrations of metal ions only the Pb^{2+} stabilized sensor has the capacity to activate fluorescence over the DFHBI concentration range tested (black). In contrast, the K^+ and Ca^{2+} stabilized sensors required much higher concentrations of DFHBI (red and blue, respectively). RNA concentration was 30 nM.

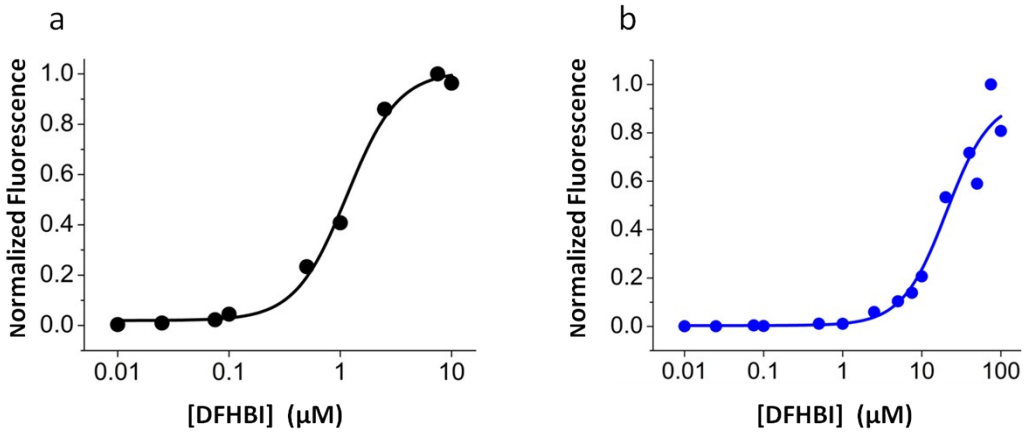

Figure S11. Binding affinity of DFHBI to Spinach in the presence of 10 μM Pb^{2+} (a) and 50 mM Ca^{2+} (b). (a) A fit of the data to the Hill equation gave an apparent K_D of 1.14 ± 0.09 μM. (b) A fit of the data to the Hill equation gave an apparent K_D of 20.45 ± 5.85 μM. RNA concentration was 30 nM in for both (a) and (b).

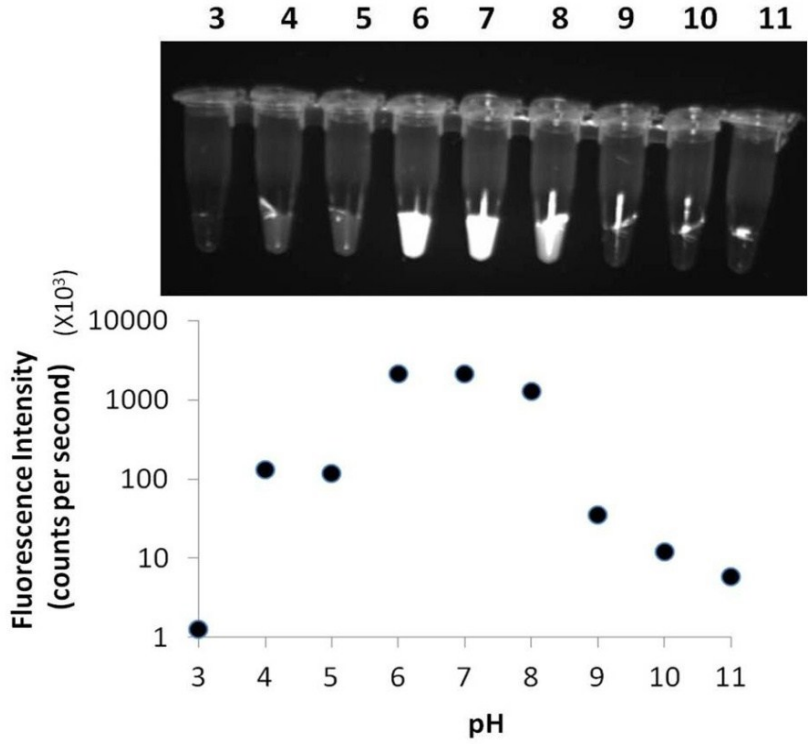

Figure S12. Activity of spinach sensor in different pH. Activity of spinach sensor was interrogated in a broad range pH 3-11. Spinach sensor shows optimal activity in the pH range 6-8. RNA and DFHBI concentrations were 5 μM and 20 μM, respectively.

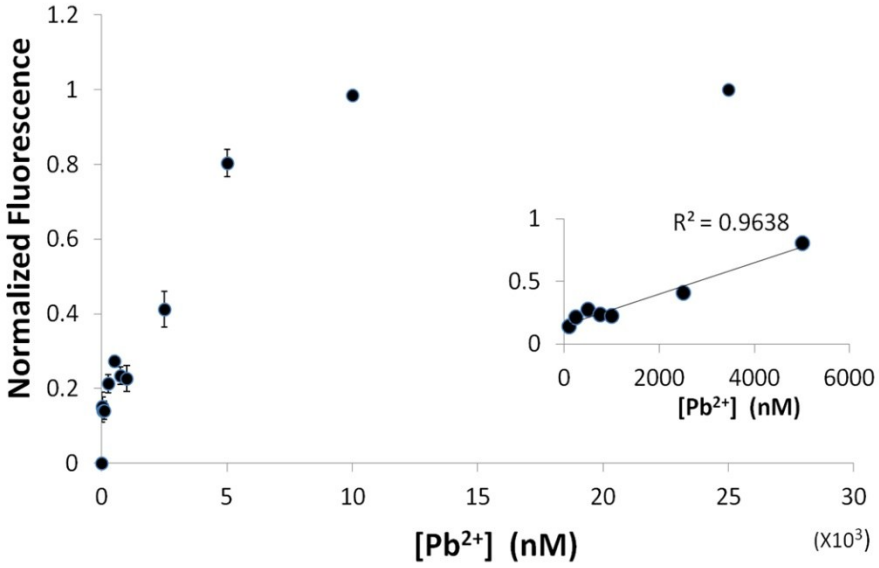

Figure S13. Spinach sensor detects lead in tap water. The sensor responds linearly (R^2=0.9638) to Pb^{2+} concentrations in the range of 100 nM-5 μM in tap water (inset). RNA and DFHBI concentrations were 100 nM and 1 μM, respectively.

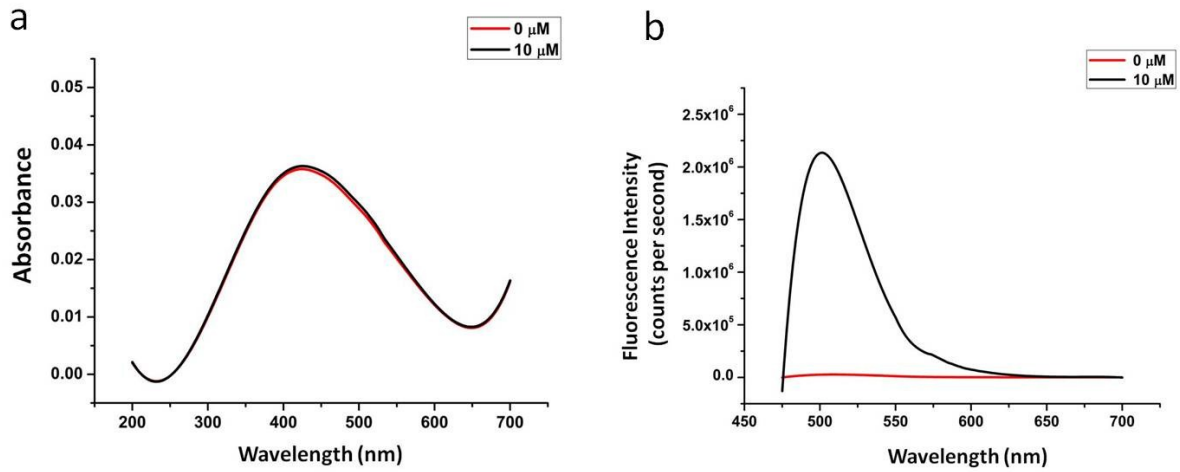

Figure S14. Absorption (a) and emission (b) spectra for the Spinach sensor in the absence (red) and presence (black) of 10 μM Pb^{2+}. (a) Absorption spectra of the sensor are identical in the absence or presence of Pb^{2+} (two spectra are superimposed on each other). (b) Emission spectra of the sensor indicate that the Spinach sensor shows enhanced fluorescence in presence of Pb^{2+}. Concentrations of RNA and DFHBI were 5 μM and 20 μM respectively